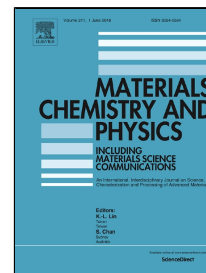# Accepted Manuscript

Effect of additive phosphorus-nitrogen containing flame retardant on char formation and flame retardancy of epoxy resin

Zhenzhong Sun, Yanbei Hou, Yuan Hu, Weizhao Hu

Please cite this article as: Zhenzhong Sun, Yanbei Hou, Yuan Hu, Weizhao Hu, Effect of additive phosphorus-nitrogen containing flame retardant on char formation and flame retardancy of epoxy resin, *Materials Chemistry and Physics* (2018), doi: 10.1016/j.matchemphys.2018.04.065

Effect of additive phosphorus-nitrogen containing flame retardant on char formation and flame retardancy of epoxy resin

Zhenzhong Sun, Yanbei Hou, Yuan Hu[*], Weizhao Hu[**]

State Key Laboratory of Fire Science, University of Science and Technology of China, 96 Jinzhai Road, Hefei, Anhui 230026, PR China

 * Corresponding author. State Key Lab of Fire Science, University of Science and Technology of China, Hefei, Anhui 230026, PR China. Tel.: +86 551 6360 1664.

** Corresponding author. Tel.: +86 551 6360 2353.

E-mail address: yuanhu@ustc.edu.cn (Y. Hu), hwz1988@ustc.edu.cn (W. Hu).

Abstract: A novel polymeric flame retardant poly(pentaerythritol phosphate phosphinic acyl piperazine) (PPAP) was synthesized successfully. The structure was confirmed by Fourier transform infrared spectra (FT-IR) and nuclear magnetic resonance spectra (NMR). The flame retardant property was characterized by limited oxygen index (LOI) and cone calorimetry test. Compared with 19% of epoxy resin, the LOI value of epoxy resin/PPAP composites (EP/PPAP) could reach high up to 35% when PPAP content was 20wt % (EP-4) and the photographs of char residues demonstrated excellent char-forming ability of PPAP. The increasing char residues in thermogravimetric analysis (TGA) and analyses of real time FT-IR (RT-FTIR) showed improved thermal stabilities of EP/PPAP composites. The formation of enhanced stable char layer were proved by FT-IR, scanning electron microscopy (SEM) and Raman spectroscopy. The dynamic mechanical properties of EP/PPAP composites such as storage modulus and crosslinking density were substantially

enhanced.

Keywords: epoxy resin; flame retardant; improvement on char formation; enhanced physical properties

1. Introduction

As a typical thermosetting material, cured epoxy resins (EP) are widely used in preparation of structural laminates, potting formulations, molding formulations because of the characteristics of toughness, low shrinkage, high adhesion to substrates and versatility in formulation [1-2]. While epoxy resins are easy to be burned comparing with metal materials, advanced epoxy resins are particularly useful for circuit boards application where flame retardant property is strictly required because of the electrical insulating properties [3]. Halogenated compound which are often used as comonomer or additive for epoxy resins have pretty good effect on flame retardancy, but combustion of halogen-containing materials will produce a lot of poisonous and high-temperature smoke, leading to a negative influence on environment development and human health [4-6]. So research and development of halogen-free flame retardants have been a hot area in recent years.

Among the developing flame retardants, organophosphorus compounds have demonstrated good ability as flame retardants for polymer materials due to low toxicity, less smoke and high flame-retardant efficiency [7-9]. As a result of the synergistic flame retarding effect between phosphorus and nitrogen components in flame retardants, flame retardants containing phosphorus and nitrogen can impart better flame retardant to epoxy resins [10-12].During combustion, as acid precursors in condensed phase,

phosphorus added in polymer catalyzes carbonization of polymer substrate to yield an intumescent physical barrier to heat radiation transfer and to diffusion of combustible gases. Besides, in gas phase, phosphorus takes effect as an efficient radical scavengers to impede combustion by the quenching mechanism [13, 14]. The nitrogen-containing compounds can decompose to nitrogenous nonflammable gasses such as nitrogen or ammonia, which will dilute oxygen concentration at the substrate-flame interface, reducing development of flame and increasing the possibility of self-extinguishment. The nitrogenous gases can also promote the expansion of char layer to create a thicker foamy carbon barrier with the synergistic effect of phosphorus [15]. Therefore, addition of components containing phosphorus and nitrogen into a flame retarding agent to increase the amount of char residue is a considerable way to obtain high flame retardant efficiency. Among the developing flame retardant additives, research of polymeric flame retardants have aroused widespread interest due to their good thermal stability, high charring ability and low effect on mechanical properties [16-18].

In this article, the aim of the research is principally about synthesizing a kind of polymeric flame retarding additive to promote formation of the intumescent protective char layer. As has been widely reported, the main function of char layer is delaying the volatilization of decomposition products and trapping decomposition products through chemical reaction as a mass transport barrier [19]. It has been proved that caged bicyclic phosphates and their derivatives can serve as effective intumescent flame retardants [20-21]. The caged bicyclic phosphate 2,6,7-trioxa-1-phosphabicyclo[2.2.2]octane-4-methanol (PEPA) is worth considering as component of ideal flame retarding additive

for its high thermal stability and excellent char-forming capacity. For nitrogen-containing segments, piperazine is often used as synthesized materials for its high reactivity, good thermal stability and char-forming capacity [22]. In this research, a novel polymeric flame retardant additive containing both PEPA and piperazine structure was synthesized successfully. After the structure was characterized distinctly, the thermal stability, flammability and flame retardant mechanism of epoxy resins incorporated with different content of flame retarding additive were tested and effect of additive on physical properties was investigated in detail.

2. Experimental

2.1. Materials

Phosphorus oxychloride ($POCl_3$) was provided by Shanghai Aladdin Bio-chemical Technology Corporation (Shanghai, China), and distilled before use. Triethylamine, acetonitrile, pentaerythritol, diaminodiphenylmethane (DDM) and anhydrous piperazine were purchased from Sinopharm Chemical Reagent Co., Ltd., China. Diglycidyl ether of bisphenol A (DGEBA, E-44, epoxy value = 0.44 mol/100 g) was obtained from JIADIDA Chemical Corporation. Pentaerythritol phosphate (PEPA) was prepared according to the ref. 23 and recrystallized in alcohol. Triethylamine and acetonitrile were purified to remove water by distillation over CaH_2 before use.

2.2. Synthesis of poly(pentaerythritol phosphate phosphinic acyl piperazine) (PPAP)

In a 500 ml four-necked glass flask equipped with a thermometer, a mechanical stirrer, a reflux condenser and a nitrogen inlet, 15.3 g of $POCl_3$, 18 g of PEPA and 200 ml acetonitrile were blended. The mixture was heated to 80 °C and stirred for 8 h under

nitrogen atmosphere. After concentration and rotary evaporation, the intermediate was obtained. In a three neck glass flask, the intermediate (22.75 g) was dissolved in 200 ml acetonitrile, then a solution of 8.6 g of anhydrous piperazine in 150 ml acetonitrile was added dropwise into the mixture which was cooled in an ice bath. The reaction mixture was heated to 40 °C after stirring for 2 h. Then 20.2 g of triethylamine was slowly added into the flask, after that, reaction was kept at 80 °C for 6 h. The mixture was filtrated and washed with water several times to remove triethylamine hydrochloride. A white solid was obtained after dried in a vacuum oven at 100 °C for 12 h, the yield was 81%.

2.3. Preparation of EP and EP/PPAP composites

EP/PPAP composites were prepared as follows: DGEBA and PPAP (0, 5, 10, 15, 20wt % of the total thermosets) were stirred fully in a three-necked flask equipped with a mechanical stirrer at 100 °C to get various homogenous blends for 10 h. The stoichiometric DDM referred to DGEBA was dissolved and added. The mixture was poured into molds after stirring for 30 s to mix DGEBA with cross-linking agent thoroughly. Then it was cured at 100 °C for 2 h and post-solidified at 150 °C for 2 h. After that, specimens were gradually cooled to room temperature to avoid stress cracking. The PPAP contents in the EP composites are listed in Table 1.

2.4. Measurements and characterizations

Nuclear magnetic resonance spectra (NMR) were obtained on a Bruker AV400 NMR spectrometer (400 MHz) at room temperature. The test samples were all dissolved in d-DMSO, the internal standard for ^{1}H NMR spectra was tetramethylsilane and the

external standard for ^{31}P NMR was 85% phosphoric acid.

Fourier transform infrared spectra (FT-IR) were measured by a Nicolet 6700 spectrometer (Nicolet Instrument Co., USA). All the samples were mixed with KBr and pressed into flakes.

Dynamic mechanical analysis (DMA) was performed on a DMA Q800 apparatus (TA Instruments Inc., USA) from 25 to 225 °C at a heating rate of 5 °C/min. The dimensions of samples were $35 \times 10 \times 3$ mm^3 with a measuring frequency of 1 Hz.

Thermogravimetric analysis (TGA) was measured with a Q5000 thermal analyzer (TA Co., USA) under nitrogen and air atmosphere from room temperature to 800 °C at a heating rate of 20 °C/min.

Limited oxygen index (LOI) was conducted on a HC-2 oxygen index meter (Jiang Ning Analysis Instrument Co., China) according to ASTM Standard D2863 with sample dimensions of $100 \times 6.5 \times 3$ mm^3.

Vertical burning test (UL-94) was performed on a CZF-II vertical burning tester (Jiang Ning Analysis Instrument Co., China). The dimension of test samples was 130 $\times 13 \times 3$ mm^3 according to ASTM D3801.

Cone calorimetry test was carried out on a cone calorimeter (Fire Testing Technology, UK) under a heat flux of 35 kW/m^2. The dimension of measured samples was $100 \times 100 \times 3$ mm^3 according to ISO Standard 5660.

Scanning electron microscopy (SEM) micrographs were obtained on a FEI Sirion 200 scanning electron microscope at an acceleration voltage of 10 kV in vacuum environments.

Real time FT-IR was collected on the Nicolet 6700 FT-IR spectrophotometer equipped with a ventilated oven with an additional heating device. The samples were heated at a rate of 10 °C/min after mixed with KBr powder and pressed into flakes.

Raman spectra in the range of 800-1800 cm^{-1} were conducted on a LabRAM-HR Confocal Raman Microprobe (JobinYvon Instruments, France) with a 514.5 nm argon ion laser.

3. Results and discussion

3.1. Characterization of PPAP

The structure of PPAP is characterized by ^{1}H NMR and ^{31}P NMR. Fig. 2 shows that the chemical shifts at 4.7 ppm and 4.6 ppm corresponded to those three CH$_2$ protons in caged bicyclic phosphate and the CH$_2$ proton close to cage structure, respectively. The resonance of CH$_2$ protons on piperazine ring appears at 2.9 ppm [24]. For ^{31}P NMR spectrum shown in Fig. 3, comparing with the peaks at 7.7 ppm attributed to the phosphorus of phosphamide ester in the main chains，the chemical shifts of phosphorus at end of polymer chains were shifted to -1.1 ppm and 14.3 ppm owing to the morphological change of phosphorus resulted from the different amount of adjacent oxygen atoms. The strong and sharp peak at -7.5 ppm is related to the phosphorus in the caged bicyclic phosphate.

From FT-IR spectrum displayed in Fig. 4, there is a broad absorption peak at 3433 cm^{-1} related to the stretching vibration of O-H, the medium peaks at 1634 and 1465 cm^{-1} are contributed to the scissoring vibration of C-H on saturated CH$_2$.The sharp peak at 1200 cm^{-1} is associated with the stretching vibration of P=O. The peaks corresponded

to stretching vibration brands of P-O-C [25-27] and P-N [27, 28] are at 1024 and 970 cm^{-1}, respectively. Both NMR and IR results demonstrate the expected structures of PPAP.

3.2. Flame retardant property of EP and EP/PPAP composites

The flame retardancy of thermosets are measured through LOI test, vertical burning test and cone calorimetry. From the collected results, it can be concluded that after incorporating PPAP with epoxy resin, great flame retarding property can be obtained, which can be attributed to the formation of an intumescent char barrier during combustion.

3.2.1. Flammability characteristic of EP and EP/PPAP

LOI is defined as the minimum concentration of oxygen in a flowing mixture of oxygen and nitrogen, which can supports downward flame combustion of samples [29, 30], it is widely used as flammability characterization of polymer materials. As can be seen from Table 1, LOI value of EP-4 is as high as 35%, which is higher than the oxygen concentration in the air, showing that EP-4 will be nonflammable. Fig. 5 shows the photographs of char residues after LOI test. It is well known that a high-quality and continuous residual char can significantly reduce air infiltration and heat conduction from fire to substrate matrix. For EP, char residue of EP is flocculent and easy to be broken without any intumescence. However, the residue of EP-4 can expand doubled and the surface shows an obvious metal-like luster, indicating the graphitization of char layer, which means better protective effect against release of combustible gases and conduction of heat radiation. The flammability and char-forming ability of PPAP is

further researched by cone calorimetry.

3.2.2.   Analysis of cone calorimetry

Due to the circumstance similar to real fire, cone calorimetry has been an efficient method to simulate a realistic fire scenario and provide a comprehensive flame retardant characterization in the research of novel flame retardants [31, 32]. The time to ignition (TTI) can be used to confirm the influence of flame retardants on ignitability. The recorded parameters such as heat release rate (HRR) and total heat release (THR) could provide crucial information of flammability. The detailed parameters including TTI, HRR, average HRR (AHRR) and the amount of residue char are given in Table 2.

As Table 2 shows, TTI value of EP is higher than EP/PPAP composites, one reason for these phenomenon may be the advanced decomposition of PPAP, which is corresponded to the TGA results. The degradation products of PPAP such as phosphoric and poly-/pyro-phosphoric acids can induce the dehydration and further decomposition of EP matrix [33-35, 40].

The HRR and THR spectra are shown in Fig. 6(a) and Fig. 6(b) respectively. As can be seen, the two peaks on HRR curves indicates that there is a typical intumescent effect during the combustion. For EP-4, the first peak is related to the ignition and spread of fire on surface. HRR curve demonstrates that the second growth is corresponded to surface burning and formation of intumescent char layer. Referring to Table 2, the peak values of HRR (PHRR) and THR values of EP/PPAP composites have a significant decrease compared with EP. Moreover, PHRR value of EP-4 decreases to 416 kW/m^2, which has fallen by 70%. THR value of EP-4 is only 44.5 MJ/m^2, much lower than that

of EP, which is in accordance with the results of HRR.

Fig. 7 displays the photographs of char residues after cone calorimetry, it is obvious that PPAP can improve the volume and quality of char residue remarkably, which can also be proved by Table 2. Only 10.3wt % of porous and incomplete char residue of EP is left over. For EP-1, not only does the weight of residual char go up to 31.3wt %, but the compact char residue can be obtained. With further increase of PPAP content, much more compact residue char is left. EP-4 has residual char that weigh up to 92.7wt %, and the volume is more than double compare to that of EP-2. Considering the analysis of residues after LOI test, it can be concluded that PPAP is effective in promoting formation of intumescent char layer and fire-proofing, which is in accordance with the results of LOI test and vertical burning test.

3.3. Thermal stabilities and thermal oxidative degradation analyses

3.3.1.　Thermal stabilities analysis of PPAP and EP/PPAP composites

The thermal stabilities of PPAP and EP/PPAP composites are evaluated by TGA under air and nitrogen atmosphere. TGA spectra and DTG spectra are shown in Fig. 8 and Fig. 9 respectively. The relevant thermal degradation data such as the temperature at which the initial 5wt % mass loss occurs (T_{onset}), the temperature at maximum mass loss rate (T_{max}) and the residue mass (Char) at 800 °C are summarized in Table 3.

From TGA spectrum of PPAP displayed in Fig. 8(a), there is a decomposition process before 130 °C, the earliest mass loss may be related to the evaporation of inner water. As for DTG curves shown in Fig. 9, there is a classic one-step decomposition peak represented under nitrogen atmosphere [36], while a two-step process under air. The

second degradation stage under air may be corresponded to the thermo-oxidative degradation of char layer and formation of residual char.

It is noticed that T_{onset} and T_{max} of EP/PPAP composites are lower than EP, furthermore, the increase of PPAP content leads to the decrease of T_{onset}. Nevertheless, the residual char yield of EP-4 is high up to 28.0wt % and 4.7wt % under nitrogen and air atmosphere, respectively, which have an over 100% increase than that of EP. These phenomenon may be attributed to the lower stability of O=P-P than the C-C bond [27, 37], and the early decomposition products like phosphate groups and phosphorus/poly-/pyro-phosphorus acids degraded from phosphorus-containing groups can catalyze the inner decomposition and carbonization [33, 38-40]. The formed char layer is in form of a crosslinked carbon-phosphorus structure [41]. It is inferred from these analytical results that the incorporation of PPAP have a reinforcing effect in condensed phase to promote charring of thermosets.

3.3.2.   Thermal oxidative degradation analysis of EP and EP/PPAP composite

RT-FTIR test can provide the intuitive information of the chemical structure change of EP and EP/PPAP composite in condensed phase during thermal oxidative degradation，it is easy to further understand the thermal degradation and char-forming process from those results. Fig. 10 and Fig. 11 exhibit the RT-FTIR spectra of EP and EP-4 at different temperature, respectively.

As for EP, the characteristic absorption peaks of epoxy resin such as benzene rings and saturated alkanes can be clearly distinguished at room temperature. The broad absorption peak of -OH at 3413 cm^{-1} vanishes at 240 °C, indicating the release of water.

The sharper peak at 3589 cm^{-1} corresponded to -NH appears at the same temperature, and fades away with temperature rising to 370 °C, this may be caused by the release of amine-containing gases [42, 43]. While the intensities of peaks of aromatic components (1602, 1508, 832 cm^{-1}) have no significant change and the same goes for peaks related to alkyl-aryl ethers and alkyl ethers (1240, 1182, 1095 and 1024 cm^{-1}) before 370 °C [39, 44, 45], indicating that aryl structures of EP is in steady state. While saturated alkanes in EP including -CH$_3$, -CH$_2$- (2962-2825 cm^{-1}) and -C(CH$_3$)$_2$- (1400-1340 cm^{-1}) weaken apparently with rise of temperature and disappear thoroughly at 370 °C [39]. All these changes demonstrate that the structure of EP has already been destroyed when temperature rises to 370 °C, which can also be confirmed by the fact that maximum peak of DTG curve of EP appears at 370 °C. The curve of EP has been smooth at 370 °C, and all the characteristic peaks can't been discerned at temperature higher than 370 °C, which indicate the breakdown of total structure and formation of residual char.

It is clear that there is a similar alteration happens to the characteristic absorption peaks of epoxy resin in Fig. 10. The difference between the two spectra is that the characteristic absorption peaks of EP-4 disappear at 320 °C, lower than that of EP. This phenomenon indicates that incorporation of PPAP accelerates the thermal decomposition of epoxy resin matrix, which is in consistent with the analyses of cone calorimetry and TGA. It is worth noting that the symmetric and asymmetric stretching vibration of P-O-P band (1088, 882 cm^{-1}), the stretching vibration of P=O (1280 cm^{-1}) and the stretching vibration of P-O-C$_{Ar}$ (1015 cm^{-1}) appear at 370 °C, indicating the compact char layer crosslinked by the P-O-P groups and P-O-C$_{Ar}$ groups which link

with aromatic and polyaromatic structure [24, 46]. The existence of poly-nuclear aromatic structure in char layer can be supported by presence of the absorption peak of C_{Ar}-H (750 cm^{-1}) at higher temperature range [47]. With existence of crosslinked phosphorus-aromatic structures, the reinforced char layer can be obtained after combustion. The analysis is consistent with result that the second stable stage in DTG curves of EP-4 at temperature range from 380 °C to 460 °C. Another notable phenomenon is that the absorption peak of ether components (1080 cm^{-1}) can still be distinguishable at temperature higher than 370 °C, demonstrating that the thermal oxidation of alkyl and aromatic carbon leads to the formation of char layer containing more C-O structure [43, 48]. These heat-resistant components will help to form a compact char layer during combustion to separate fire.

3.4. Analyses of char residues after cone calorimetry

The barrier and protective property of char layer depend on the physical and chemical structure, to investigate the formation of char layer and flame retardant mechanism, three typical method are used to investigate the charring structure. SEM is used to analyze the surface morphology of char residues after cone calorimetry. Raman spectroscopy is a powerful tool to analyze carbonaceous structure due to its high sensitivity to the structural disorder [49, 50]. The chemical components of char residue are determined by FT-IR spectroscopy.

3.4.1. Morphology investigation of char residues

The SEM micrographs of the char residues collected from EP and EP/PPAP composites after cone calorimetry. In Fig. 12(a), there are many holes and cracks on

the fragile and fragmented surface of residual char of EP. The release of gases during combustion breaks the skeleton of char layer, leading to the formation of caves and disabling the barrier function. For EP-1, the significant improvement of the surface integrity can be demonstrated by Fig. 12(b). The surface becomes spongy with some observable gullies resulted from the gas flows, indicating that a more perfect char layer has been formed. Such a char layer can slow down the gases release and restrict thermal conductivity of heat flow from fire to inner matrix. With PPAP content reaching up to 10wt %, a denser grassy char layer with some stick-like protuberances is obtained. These protuberances may be caused by the barrier effect on release of inner gases. This speculation can be confirmed by the morphological analysis of residue char of EP-4. Fig. 12 (d) shows that there are more closed pores on the layer surface, indicating that the char layer can act as a better barrier against the release of combustible gases and the conductivity of thermal radiation. The enormous closed pores can also improve the thermal stability of char layer. All the results can be explained by the fact that the incorporation of PPAP enhances the stability of char layer, which efficiently reduce the combustion heat demonstrated in cone calorimetry.

3.4.2.   Raman spectroscopy analysis of char residues

As an effective characterization method of graphitization degree, Raman spectroscopy is used to research the physical structure of char residues after cone calorimetry. From Raman spectra displayed in Fig. 13, two characteristic band at 1360 (D band) and 1580 cm^{-1} (G band) can be distinctly distinguished, D band is related to disordered carbon structure, and G band is associated with the C-C vibration mode in

organized graphitic structure [50-53]. The intensity ratio of D bands and G bands (I_D/I_G) called R is corresponded to the microcrystal size of char layer and is widely used for the characterization of graphitization degree, where I_D and I_G are the integrated intensities of the D and G bands, respectively. It has been reported that the R value is inversely proportional to the microcrystalline size [52-56]. The larger R value demonstrates the smaller microcrystalline carbonaceous structure and smaller pore diameter of char layer, which means the better protective efficiency [53, 54, 57]. According to Fig. 13, the R value follows the sequence of EP (2.76) < EP-1 (2.79) < EP-2 (2.92) < EP-4 (3.95), illustrating the improvement in thermal stability and heat insulation of char layer obtained by PPAP.

3.4.3.   FT-IR research of char residues

The carbon residues of thermosets after cone calorimetry are measured by FT-IR spectroscopy to further investigate the chemical structure of char layer. From FT-IR spectra shown in Figure 14, the absorption peaks at 1584 and 1396 cm^{-1} are related to carbonaceous network structures such as aromatic and poly-nuclear aromatic components formed at later burning stage [42, 59]. For EP/PPAP composites, it is worth noting that with increase of PPAP content, the intensity of characteristic peaks attributed to P-O-C (976 cm^{-1}) and P-O-P (1082 cm^{-1}) increase, the absorption peak corresponded to P=O (1230 cm^{-1}) reduces on the contrary. It can be illuminated by these phenomenon that there are more crosslinked phosphorus-carbonaceous and phosphorus-oxidative structures in the residual chars. The phosphorus-linked structures can link to different aromatic species to promote the thermal stability and formation of

the phosphorus-rich char layer [27, 42, 58].

Considering the above analyses on physical and chemical structure of char residues, it is concluded that utilization of PPAP in epoxy resin can greatly enhance the thermal stability, promoting formation of char layer with more phosphorus-crosslinked structure and smaller microcrystalline dimension. The improved char layer efficiently insulates substrate against heat radiation and prevents combustible gases from reaching the fire, which leading to the great flame retardant performance of EP/PPAP thermosets.

3.5. Dynamic mechanical properties of EP/PPAP composites

DMA provides the variations of storage modulus (E') and loss factor (tanδ) with temperature, which can be used to characterize viscoelastic properties of epoxy resins. The storage modulus is related to the load bearing capacity of materials. The glass transition temperature (T_g) is defined as the peak of tanδ curve. The E' and tanδ curves are plotted in Fig. 15 and Fig. 16 respectively. As can be seen from Fig. 16, T_gs of EP/PPAP composites increase with the increase of PPAP content in general. Most spectacularly, T_g of EP-4 rises by about 15% compared with that of EP.

The crosslinking density (V_e) of EP/PPAP composites is defined by the following equation according to the rubber theory of elasticity [60-63]:

$$V_e = E'/3RT$$

In this equation, E' is the storage modulus at rubbery plateau (Tg + 40 °C) shown in Table 4, R is the ideal gas constant and T is the absolute temperature at Tg + 40 °C. From results listed in Table 4, the addition of PPAP results in the increase of E' at rubbery plateau, suggesting that PPAP to a certain extent has an enhancement on the

dynamic modulus. And it is clearly that crosslinking density has significant growth after incorporating PPAP into the EP matrix, which may be cause by the strong interfacial adhesion of the cured EP matrix and PPAP [64, 65]. For thermosets, it should be knew that crosslinking density not only is the affected factor of mechanical properties, but is advantageous to flame retardant efficiency [66]. As for EP-4, the high flame retardancy will be obtained since the evident increased crosslinking density.

4. Conclusions

A novel intumescent polymeric flame retardant additive containing phosphorus and nitrogen named PPAP is successfully synthesized. The ^{1}H, ^{31}P NMR spectroscopy and FT-IR spectroscopy characterize the structure of PPAP clearly. After incorporation with epoxy resin, the EP/PPAP thermosets show better thermal stability and thermal oxidative stability which are demonstrated by TGA and RT-FTIR measurements. The thermosets can achieve LOI value high up to 35 and UL-94 V-0 rating when 20wt % of PPAP is added. In cone calorimetry, excellent effects on improvement of char-formation and reduction of heat radiation (92.7wt % of char residue left, 70% decline of PHRR and 60% decrease of THR). PPAP is also proved to be beneficial to improvement of mechanical property by DMA. The compact phosphorus-rich char layer of EP/PPAP composites after combustion is confirmed by chemical and physical structural investigations from SEM, FT-IR and Raman spectroscopy. Such a char layer can act as an efficient barrier for inner substrate during combustion to prevent degradative gases from diffusing to fire and to protect the matrix from heat, consequently bringing about better flame retardancy of epoxy resin.

References

[1]   Chemistry and technology of epoxy resins [M]. London: Blackie Academic & Professional, 1993.

[2]   Wu C S, Liu Y L, Chiu Y C, et al. Thermal stability of epoxy resins containing flame retardant components: an evaluation with thermogravimetric analysis [J]. Polymer Degradation and Stability, 2002, 78(1): 41-48.

[3]   Lin C H, Wang C S. Novel phosphorus-containing epoxy resins Part I. Synthesis and properties [J]. Polymer, 2001, 42(5): 1869-1878.

[4]   Gu J, Zhang G, Dong S, et al. Study on preparation and fire-retardant mechanism analysis of intumescent flame-retardant coatings [J]. Surface and coatings technology, 2007, 201(18): 7835-7841.

[5]   Sun D, Yao Y. Synthesis of three novel phosphorus-containing flame retardants and their application in epoxy resins[J]. Polymer degradation and stability, 2011, 96(10): 1720-1724.

[6]   Uddin M A, Bhaskar T, Kusaba T, et al. Debromination of flame retardant high impact polystyrene (HIPS-Br) by hydrothermal treatment and recovery of bromine free plastics[J]. Green Chemistry, 2003, 5(2): 260-263.

[7]   Lu S Y, Hamerton I. Recent developments in the chemistry of halogen-free flame retardant polymers[J]. Progress in Polymer Science, 2002, 27(8): 1661-1712.

[8]   Weil E D, Levchik S. A review of current flame retardant systems for epoxy resins[J]. Journal of fire sciences, 2004, 22(1): 25-40.

[9]   Liu Y L, Hsiue G H, Chiu Y S, et al. Phosphorus-containing epoxy for flame retardant. I. Synthesis, thermal, and flame-retardant properties[J]. Journal of applied polymer science, 1996, 61(4): 613-621.

[10]   Cyriac A, Lee S H, Varghese J K, et al. Preparation of flame-retarding poly (propylene carbonate)[J]. Green Chemistry, 2011, 13(12): 3469-3475.

[11]   Liu Y L, Hsiue G H, Lee R H, et al. Phosphorus-containing epoxy for flame retardant. III: Using phosphorylated diamines as curing agents[J]. Journal of Applied Polymer Science, 1997, 63(7): 895-901.

[12]   Varma I K. Effect of structure on thermal behaviour of phosphorus containing addition polyimides and epoxy resins[J]. Materials Research Innovations, 2001, 4(5-6): 306-310.

[13]   Toldy A, Toth N, Anna P, et al. Synthesis of phosphorus-based flame retardant systems and their use in an epoxy resin[J]. Polymer Degradation and Stability, 2006, 91(3): 585-592.

[14]   Wang X, Song L, Xing W, et al. A effective flame retardant for epoxy resins based on poly (DOPO substituted dihydroxyl phenyl pentaerythritol diphosphonate)[J]. Materials Chemistry and Physics, 2011, 125(3): 536-541.

[15]   Perez R M, Sandler J K W, Altstädt V, et al. Effect of DOP-based compounds on fire retardancy, thermal stability, and mechanical properties of DGEBA cured with 4, 4′-DDS[J]. Journal of materials science, 2006, 41(2): 341-353.

[16]   Kannan P, Murugavel S C. Studies on photocrosslinkable-cum-flame retardant poly (benzylidene phosphoramide ester) s[J]. Journal of Polymer Science Part A: Polymer Chemistry, 1999, 37(16): 3285-3291.

[17]   Tai Q, Hu Y, Yuen R K K, et al. Synthesis, structure-property relationships of polyphosphoramides with high char residues[J]. Journal of Materials Chemistry, 2011, 21(18): 6621-6627.

[18]   Chen L, Wang Y Z. Aryl polyphosphonates: useful halogen-free flame retardants for polymers[J]. Materials, 2010, 3(10): 4746-4760.

[19]   Gilman J W, Ritchie S J, Kashiwagi T, et al. Fire-retardant additives for polymeric materials—I. Char formation from silica gel-potassium carbonate[J]. Fire and Materials, 1997, 21(1): 23-32.

[20]   Allen D W, Anderton E C, Bradley C, et al. Fire-retardant polymers. Polymerisation of 1-oxo-2, 6, 7-trioxa-1-phosphabicyclo [2, 2, 2] oct-4-ylmethyl methacrylate, and its copolymerisation with methyl methacrylate, styrene, and triallylcyanurate[J]. Polymer degradation and stability, 1995, 47(1): 67-72.

[21]   Halpern Y, Mott D M. Amines salts of phosphoric acid: U.S. Patent 4,480,093[P]. 1984-10-30.

[22]   Rowton R. Piperazine phosphates as fire retardants for organic polymers: U.S. Patent 3,810,850[P]. 1974-5-14.

[23]   Halpern Y, Mott D M, Niswander R H. Fire retardancy of thermoplastic materials by intumescence[J]. Industrial & Engineering Chemistry Product Research and Development, 1984, 23 (2): 233-238

[24]   Qian X, Song L, Hu Y, et al. Combustion and thermal degradation mechanism of a novel intumescent flame retardant for epoxy acrylate containing phosphorus and nitrogen[J]. Industrial & Engineering Chemistry Research, 2011, 50(4): 1881-1892.

[25]   Quittmann U, Lecamp L, El Khatib W, et al. Synthesis of a New Phosphonated Dimethacrylate: Photocuring Kinetics in Homo-and Copolymerization, Determination of Thermal and Flame-Retardant Properties[J]. Macromolecular Chemistry and Physics, 2001, 202(5): 628-635.

[26]   Song P, Fang Z, Tong L, et al. Synthesis of a novel oligomeric intumescent flame retardant and its application in polypropylene[J]. Polymer Engineering & Science, 2009, 49(7): 1326-1331.

[27]   Zhao W, Liu J, Peng H, et al. Synthesis of a novel PEPA-substituted polyphosphoramide with high char residues and its performance as an intumescent flame retardant for epoxy resins[J]. Polymer Degradation and Stability, 2015, 118: 120-129.

[28]   Jirasutsakul I, Paosawatyanyong B, Bhanthumnavin W. Aromatic phosphorodiamidate curing agent for epoxy resin coating with flame-retarding properties[J]. Progress in Organic Coatings, 2013, 76(12): 1738-1746.

[29]   Camino G, Costa L, Casorati E, et al. The oxygen index method in fire retardance studies of polymeric materials[J]. Journal of Applied Polymer Science, 1988, 35(7): 1863-1876.

[30]   La Rosa A D, Recca A, Carter J T, et al. An oxygen index evaluation of flammability on modified epoxy/polyester systems[J]. Polymer, 1999, 40(14): 4093-4098.

[31]   Schartel B, Bartholmai M, Knoll U. Some comments on the use of cone calorimeter data[J]. Polymer Degradation and Stability, 2005, 88(3): 540-547.

[32]   Zhang W, Li X, Yang R. The degradation and charring of flame retarded epoxy resin during the combustion[J]. Journal of Applied Polymer Science, 2013, 130(6): 4119-4128.

[33]   Tan Y, Shao Z B, Yu L X, et al. Piperazine-modified ammonium polyphosphate as monocomponent flame-retardant hardener for epoxy resin: flame retardance, curing behavior and mechanical property[J]. Polymer Chemistry, 2016, 7(17): 3003-3012.

[34]   Chen J, Liu S, Zhao J. Synthesis, application and flame retardancy mechanism of a novel flame retardant containing silicon and caged bicyclic phosphate for polyamide 6[J]. Polymer degradation and stability, 2011, 96(8): 1508-1515.

[35]   Qian L J, Ye L J, Xu G Z, et al. The non-halogen flame retardant epoxy resin based on a novel compound with phosphaphenanthrene and cyclotriphosphazene double functional groups[J]. Polymer degradation and stability, 2011, 96(6): 1118-1124.

[36]   Wu C S, Liu Y L, Chiu Y C, et al. Thermal stability of epoxy resins containing flame retardant components: an evaluation with thermogravimetric analysis[J]. Polymer Degradation and Stability, 2002, 78(1): 41-48.

[37]   Sun D, Yao Y. Synthesis of three novel phosphorus-containing flame retardants and their application in epoxy resins[J]. Polymer degradation and stability, 2011, 96(10): 1720-1724.

[38]   Wang Y, Zhao J, Yuan Y, et al. Synthesis of maleimido-substituted aromatic s-triazine and its application in flame-retarded epoxy resins[J]. Polymer Degradation and Stability, 2014, 99: 27-34.

[39]   Tian N, Gong J, Wen X, et al. Synthesis and characterization of a novel organophosphorus oligomer and its application in improving flame retardancy of epoxy resin[J]. RSC Advances, 2014, 4(34): 17607-17614.

[40]   Liu Y L, Hsiue G H, Lan C W, et al. Phosphorus-containing epoxy for flame retardance: IV. Kinetics and mechanism of thermal degradation[J]. Polymer Degradation and Stability, 1997, 56(3): 291-299.

[41]   Wang Q, Shi W. Kinetics study of thermal decomposition of epoxy resins containing flame retardant components[J]. Polymer Degradation and Stability, 2006, 91(8): 1747-1754.

[42]   Liu H, Wang X, Wu D. Preparation, isothermal kinetics, and performance of a novel epoxy thermosetting system based on phosphazene-cyclomatrix network for halogen-free flame retardancy and high thermal stability[J]. Thermochimica Acta, 2015, 607: 60-73.

[43]   Wang X, Hu Y, Song L, et al. Synthesis and characterization of a DOPO-substitued organophosphorus oligomer and its application in flame retardant epoxy resins[J]. Progress in Organic Coatings, 2011, 71(1): 72-82.

[44] Zhang W, Li X, Yang R. Pyrolysis and fire behaviour of epoxy resin composites based on a phosphorus-containing polyhedral oligomeric silsesquioxane (DOPO-POSS)[J]. Polymer degradation and stability, 2011, 96(10): 1821-1832.

[45] Wang X, Hu Y, Song L, et al. Flame retardancy and thermal degradation mechanism of epoxy resin composites based on a DOPO substituted organophosphorus oligomer[J]. Polymer, 2010, 51(11): 2435-2445.

[46] Bugajny M, Bourbigot S, Le Bras M, et al. The origin and nature of flame retardance in ethylene-vinyl acetate copolymers containing hostaflam AP 750[J]. Polymer international, 1999, 48(4): 264-270.

[47] Perret B, Schartel B, Stöß K, et al. Novel DOPO-based flame retardants in high-performance carbon fibre epoxy composites for aviation[J]. European Polymer Journal, 2011, 47(5): 1081-1089.

[48] Zhang W, Li X, Yang R. The degradation and charring of flame retarded epoxy resin during the combustion[J]. Journal of Applied Polymer Science, 2013, 130(6): 4119-4128.

[49] Sadezky A, Muckenhuber H, Grothe H, et al. Raman microspectroscopy of soot and related carbonaceous materials: spectral analysis and structural information[J]. Carbon, 2005, 43(8): 1731-1742.

[50] Pimenta M A, Dresselhaus G, Dresselhaus M S, et al. Studying disorder in graphite-based systems by Raman spectroscopy[J]. Physical chemistry chemical physics, 2007, 9(11): 1276-1290.

[51] Yang W, Sun W J, Chu W, et al. Synthesis of carbon nanotubes using scrap tyre

rubber as carbon source[J]. Chinese Chemical Letters, 2012, 23(3): 363-366.

[52]   Bourbigot S, Le Bras M, Delobel R. Carbonization mechanisms resulting from intumescence association with the ammonium polyphosphate-pentaerythritol fire retardant system[J]. Carbon, 1993, 31(8): 1219-1230.

[53]   Bourbigot S, Le Bras M, Delobel R, et al. Synergistic effect of zeolite in an intumescence process: study of the carbonaceous structures using solid-state NMR[J]. Journal of the Chemical Society, Faraday Transactions, 1996, 92(1): 149-158.

[54]   Tuinstra F, Koenig J L. Raman spectrum of graphite[J]. The Journal of Chemical Physics, 1970, 53(3): 1126-1130.

[55]   Knight D S, White W B. Characterization of diamond films by Raman spectroscopy[J]. Journal of Materials Research, 1989, 4(02): 385-393.

[56]   Jang B N, Wilkie C A. A TGA/FTIR and mass spectral study on the thermal degradation of bisphenol A polycarbonate[J]. Polymer Degradation and Stability, 2004, 86(3): 419-430.

[57]   Wu Q, Qu B. Synergistic effects of silicotungistic acid on intumescent flame-retardant polypropylene[J]. Polymer Degradation and Stability, 2001, 74(2): 255-261.

[58]   El Gouri M, El Bachiri A, Hegazi S E, et al. A phosphazene compound multipurpose application-Composite material precursor and reactive flame retardant for epoxy resin materials[J]. J. Mater. Environ. Sci, 2011, 2(4): 319-334.

[59] Zhang W, Li X, Li L, et al. Study of the synergistic effect of silicon and phosphorus on the blowing-out effect of epoxy resin composites[J]. Polymer degradation and stability, 2012, 97(6): 1041-1048.

[60] Henna P H, Larock R C. Rubbery Thermosets by Ring-Opening Metathesis Polymerization of a Functionalized Castor Oil and Cyclooctene[J]. Macromolecular Materials and Engineering, 2007, 292(12): 1201-1209.

[61] Francis B, Thomas S, Sadhana R, et al. Diglycidyl ether of bisphenol-A epoxy resin modified using poly (ether ether ketone) with pendent ter-butyl groups[J]. Journal of Polymer Science Part B: Polymer Physics, 2007, 45(17): 2481-2496.

[62] Flory P J. Principles of polymer chemistry[M]. Cornell University Press, 1953.

[63] Ward I M, Sweeney J. Mechanical properties of solid polymers[M]. John Wiley & Sons, 2012.

[64] Wang X, Hu Y, Song L, et al. Preparation, mechanical properties, and thermal degradation of flame retarded epoxy resins with an organophosphorus oligomer[J]. Polymer bulletin, 2011, 67(5): 859-873.

[65] Wang Q, Shi W. Photopolymerization and thermal behaviors of acrylated benzenephosphonates/epoxy acrylate as flame retardant resins[J]. European polymer journal, 2006, 42(10): 2261-2269.

[66] Zhao H B, Liu B W, Wang X L, et al. A flame-retardant-free and thermo-cross-linkable copolyester: Flame-retardant and anti-dripping mode of action[J]. Polymer, 2014, 55(10): 2394-2403.

Table 1 Formulation and flame retardancy of epoxy resin systems

Samples	EP content (wt %)	PPAP content (wt %)	LOI (%)	UL-94 rating
EP	100	0	19	No rating
EP-1	95	5.0	26	No rating
EP-2	90	10.0	28	V-1
EP-3	85	15.0	31	V-1
EP-4	80	20.0	35	V-0

Table 2 Cone calorimetry data of EP and EP/PPAP composites

Samples	EP	EP-1	EP-2	EP-4
TTI (s)	40	38	36	34
PHRR (kW/m^2)	1511.7	838.1	522.0	416.0
AHRR (kW/m^2)	162.6	105.4	75.7	62.6
THR (MJ/m^2)	115.8	75.4	54.2	44.5
Char (wt. %)	10.3	31.3	47.0	92.7

Table 3 Thermogravimetric data of epoxy resins and PPAP under N_2 and air

Samples	N_2			Air		
	T_{onset} (°C)	T_{max} (°C)	Char (%)	T_{onset} (°C)	T_{max} (°C)	Char (%)
PPAP	307	418	38.6	308	665	4.8
EP	357	374	12.9	345	370,561	0.6
EP-1	335	364	21.8	307	373,576	1.7

EP-2	323	357	24.5	311	348,584	1.1
EP-3	328	357	26.1	328	361,586	3.2
EP-4	313	336	28.0	308	336,597	4.7

Table 4 DMA results of EP and EP/PPAP composites

Samples	EP	EP-1	EP-2	EP-3	EP-4
E' (MPa)	357.2	521.2	544.3	584.2	780.4
T_g (°C)	157.0	166.2	163.9	173.4	179.8
v_e (mol/m^3)	30470.7	43607.0	45759.3	48154.5	63491.5

(PEPA)

(Intermediate)
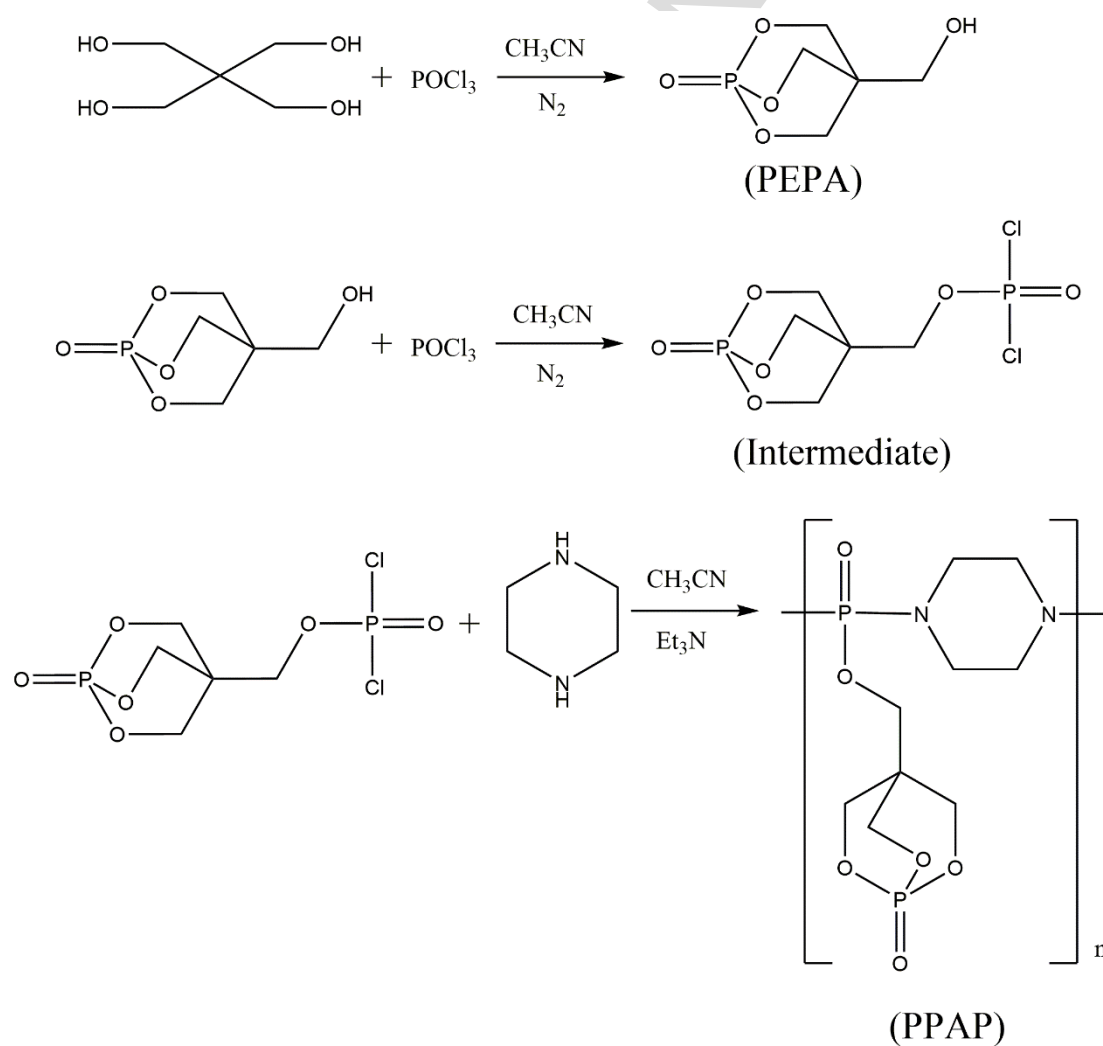
(PPAP)

Figure 1 Synthetic route of PPAP
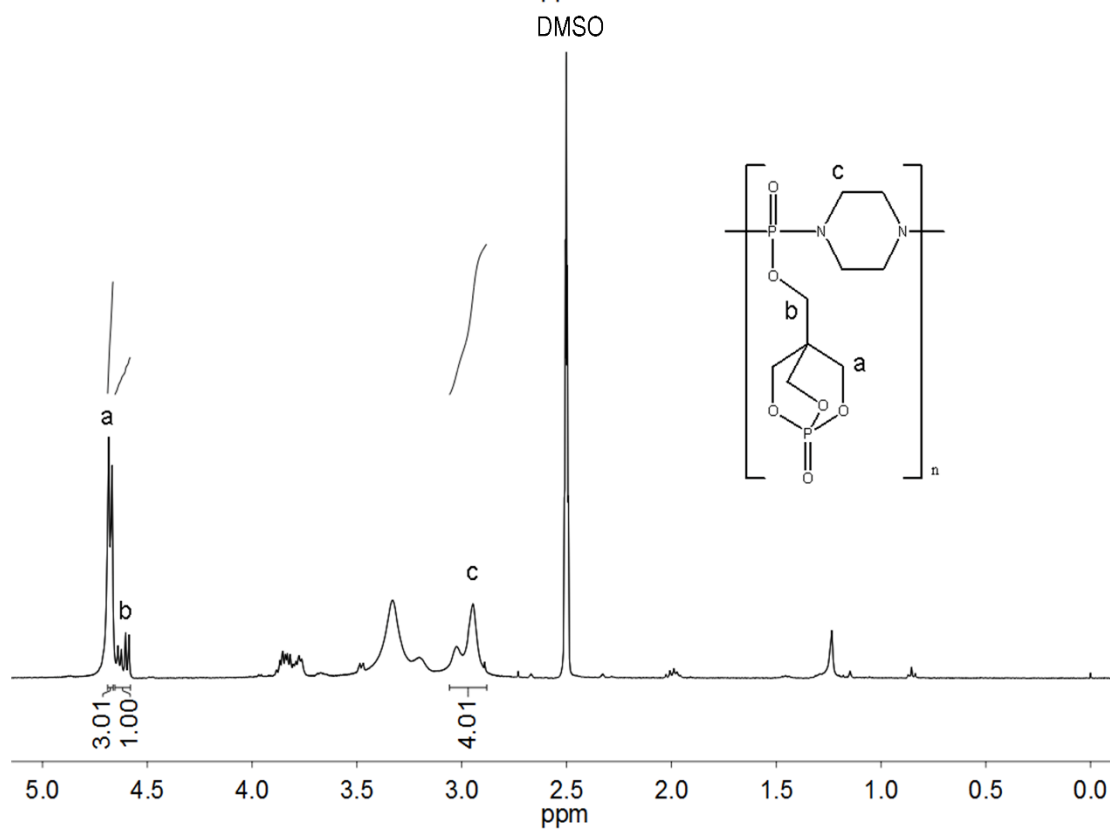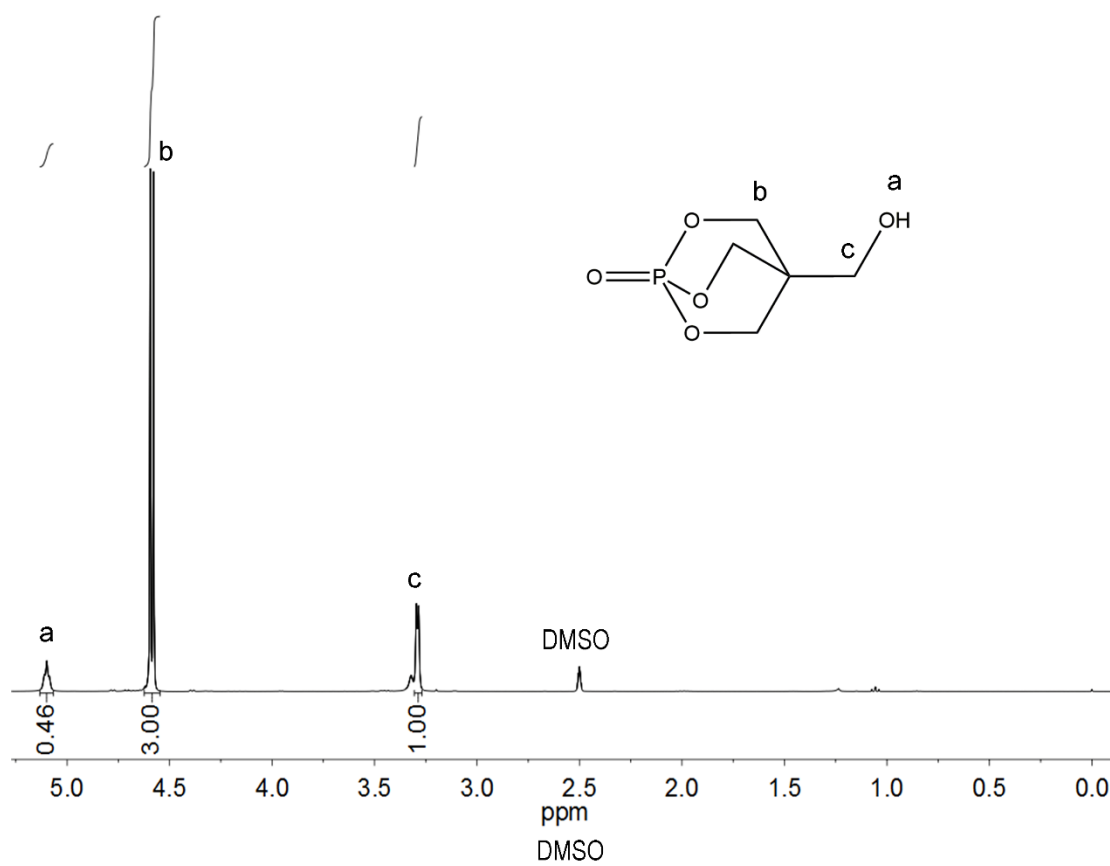
Figure 2 ^{1}H NMR spectrum of PEPA and PPAP
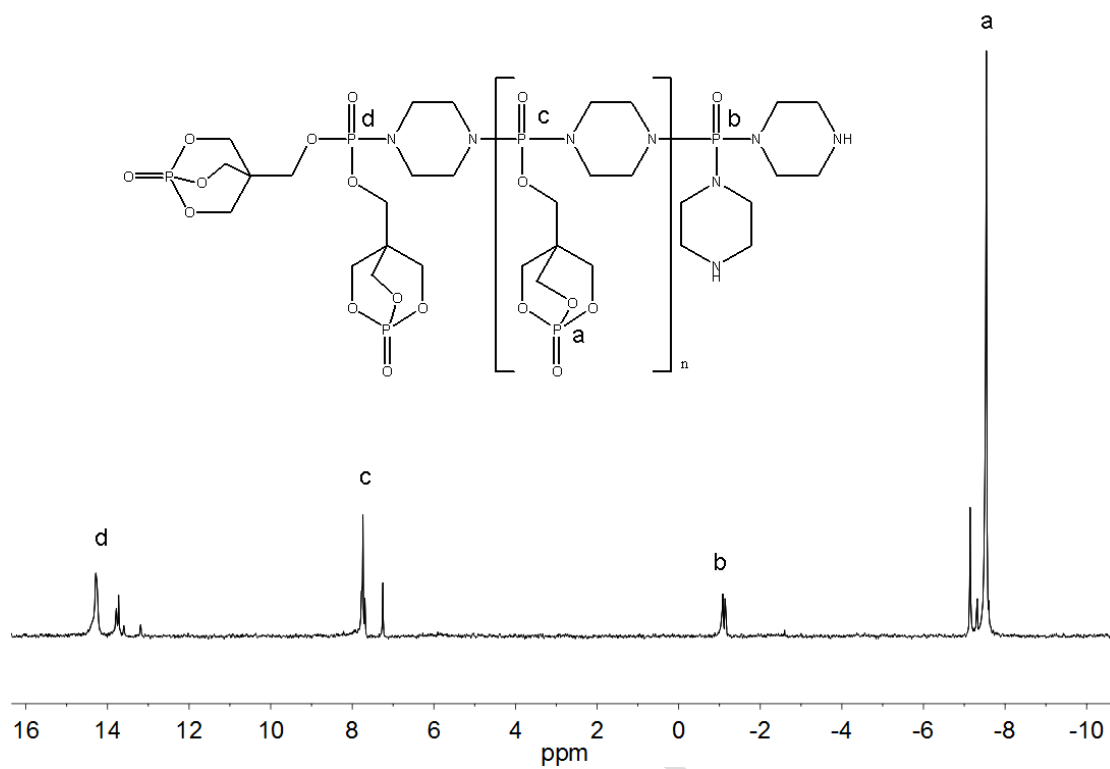
Figure 3 ^{31}P NMR spectrum of PPAP
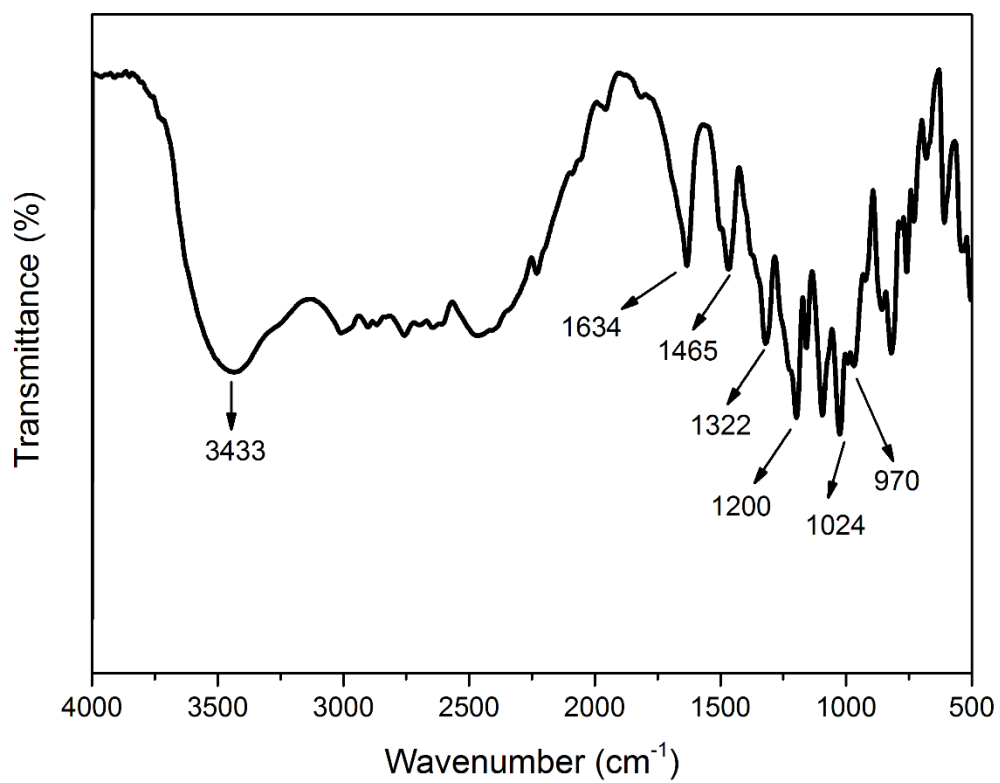
Figure 4 IR spectrum of PPAP
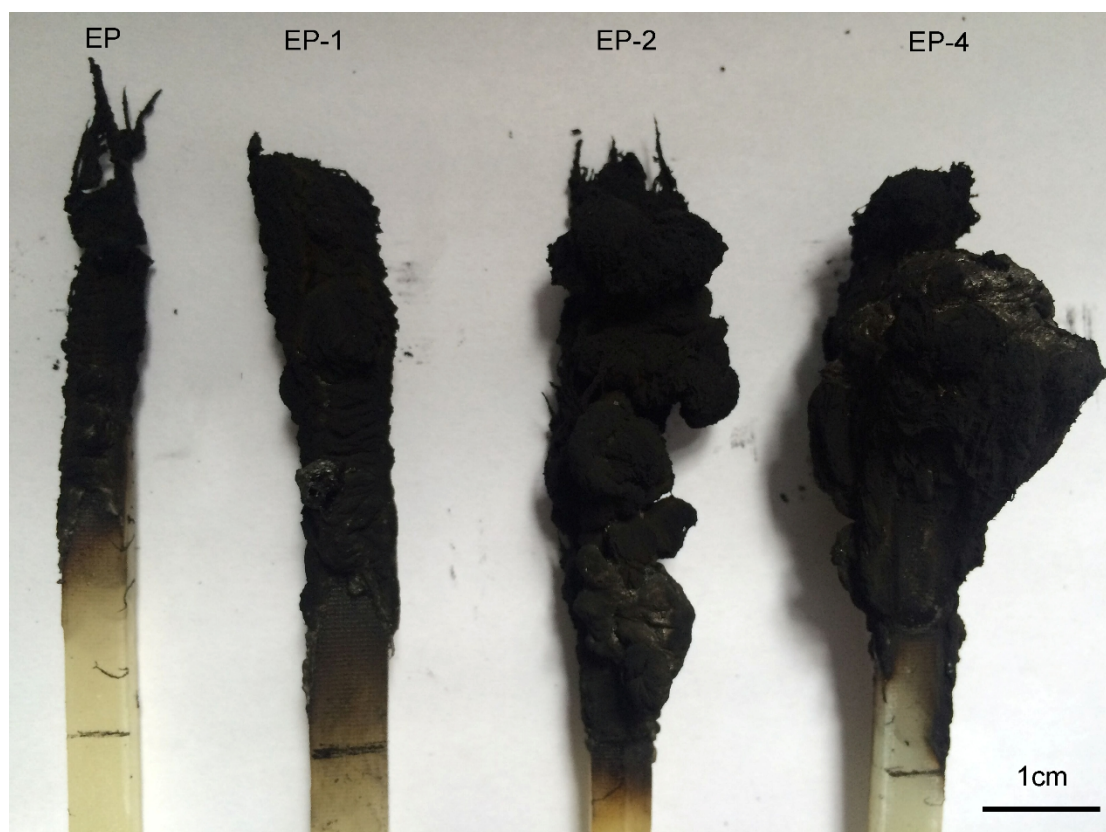
Figure 5 Photographs of thermosets after LOI test

a

b
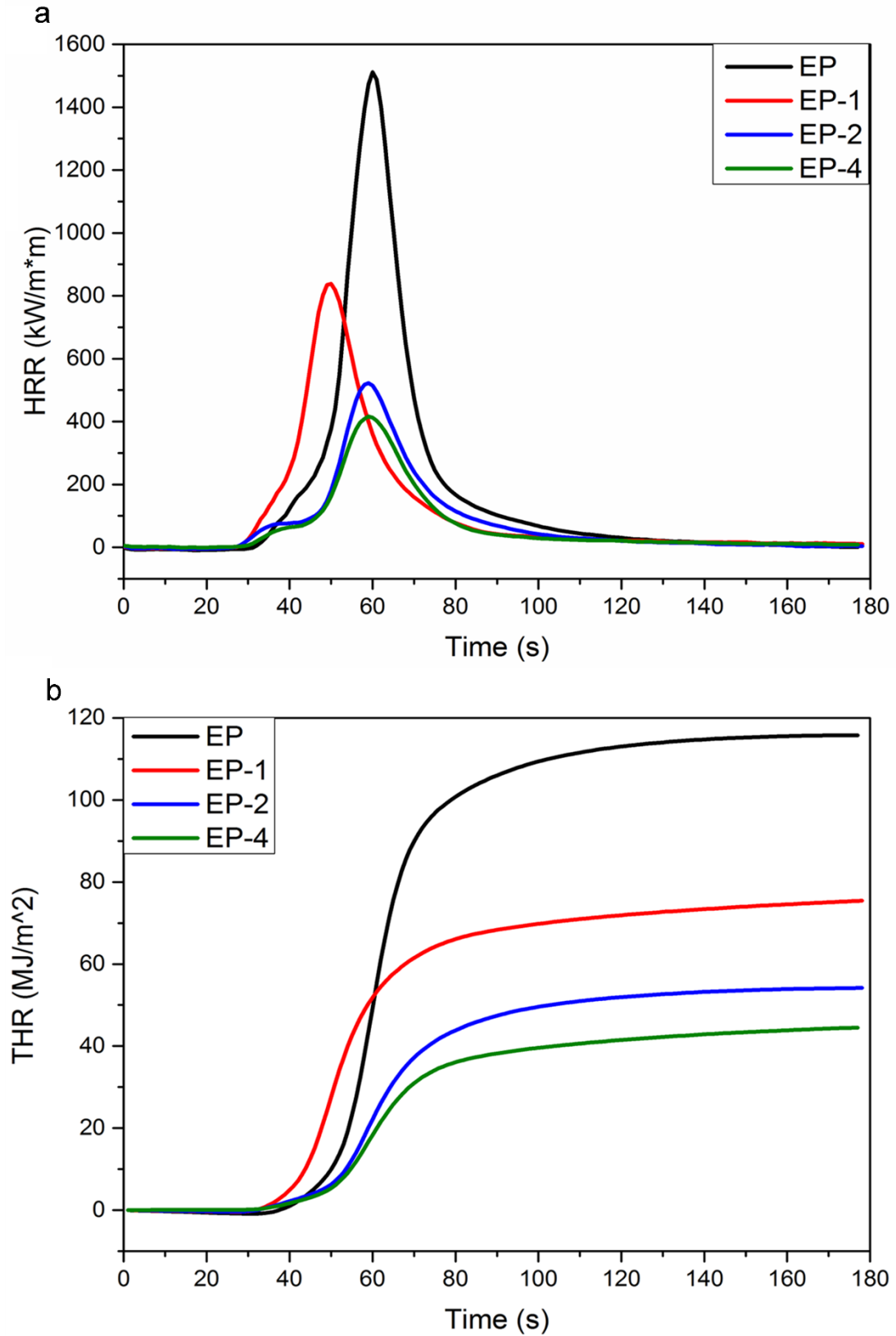
Figure 6 HRR (a) and THR (b) curves of EP and EP/PPAP composites
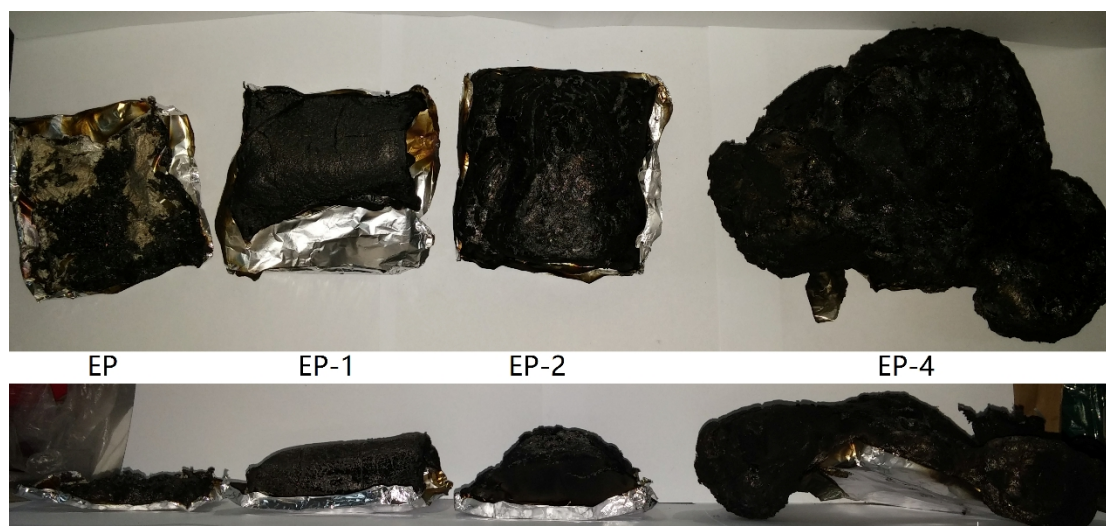
Figure 7 Photographs of the carbon residues after cone calorimetry
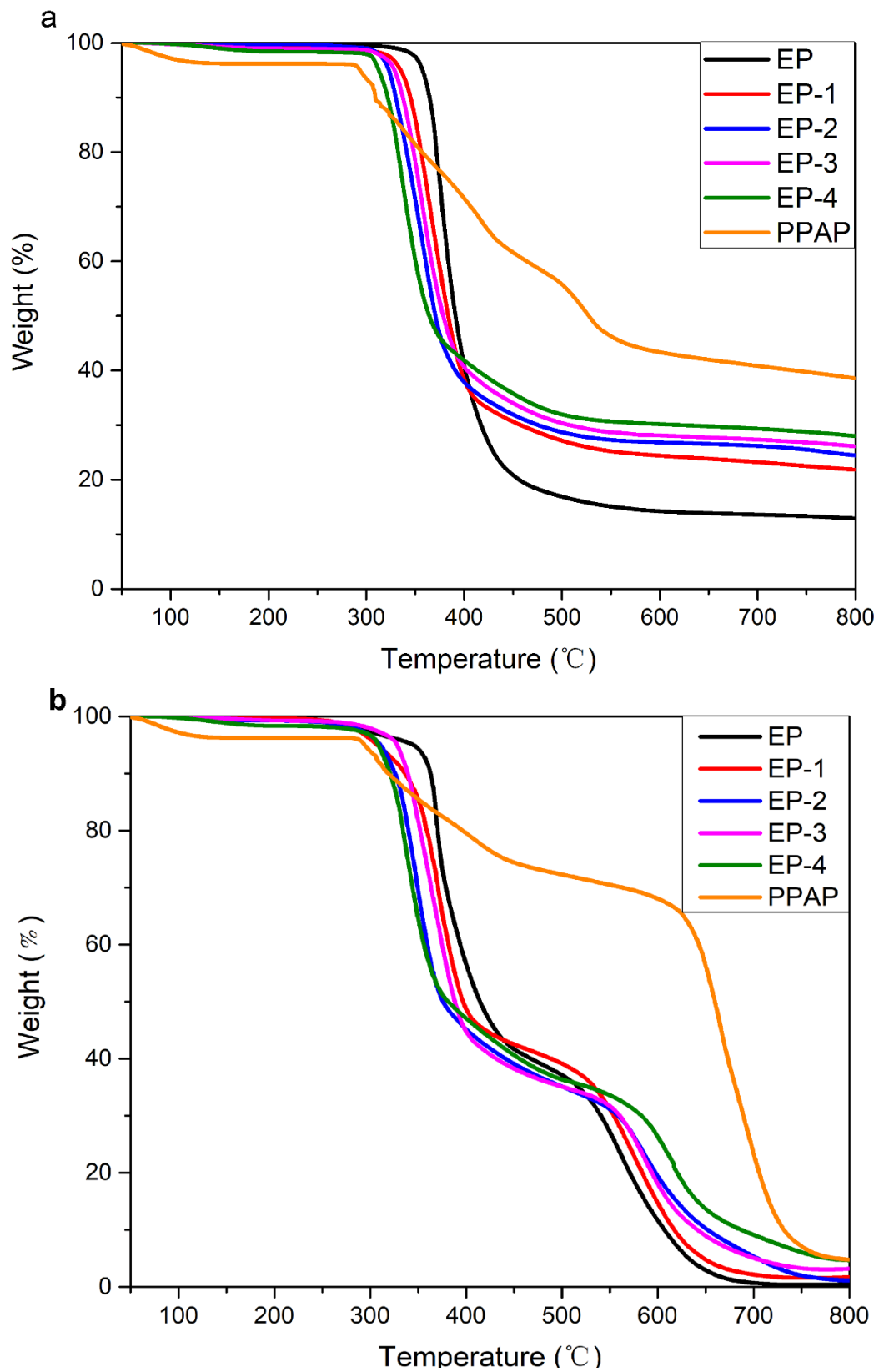
Figure 8 TGA curves of EP and EP/PPAP composites under N_2 (a) and air (b)
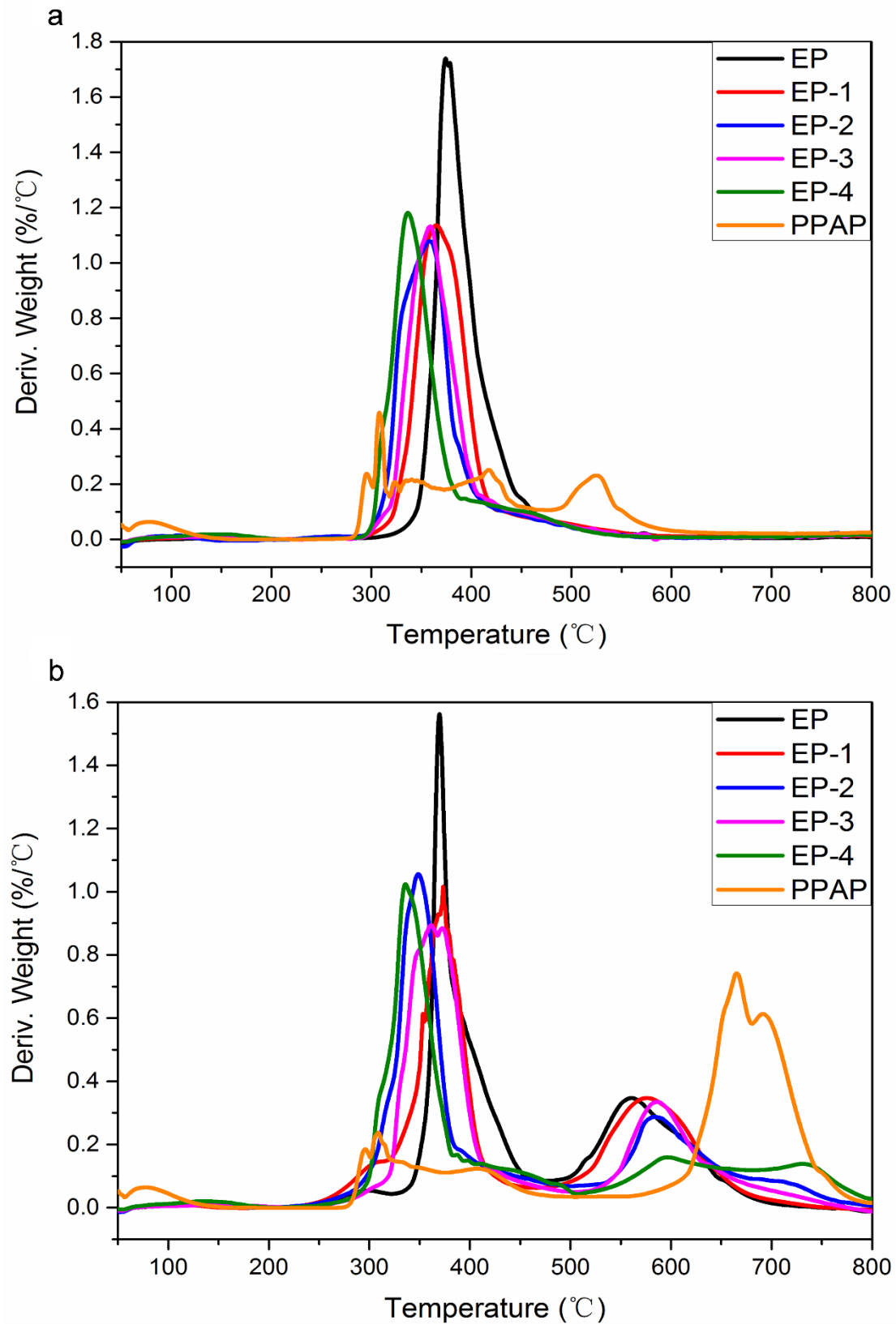
atmosphere

Figure 9 DTG curves of EP and EP/PPAP composites under N2 (a) and air (b)

atmosphere
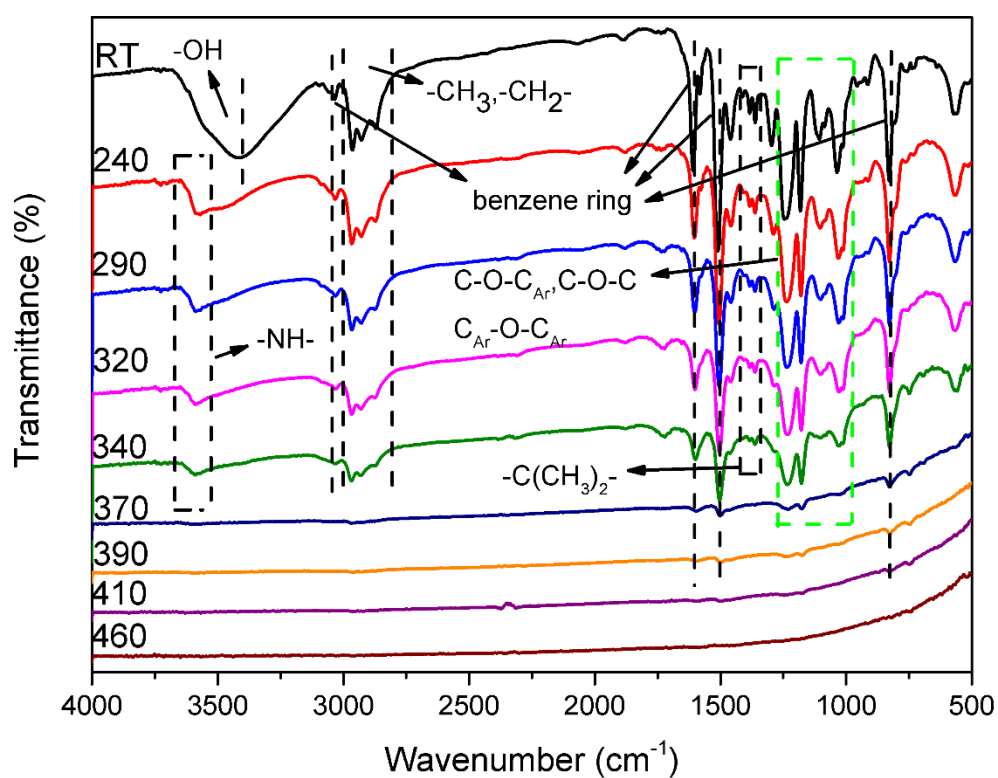
Figure 10 RT-FTIR spectra of EP at different temperature
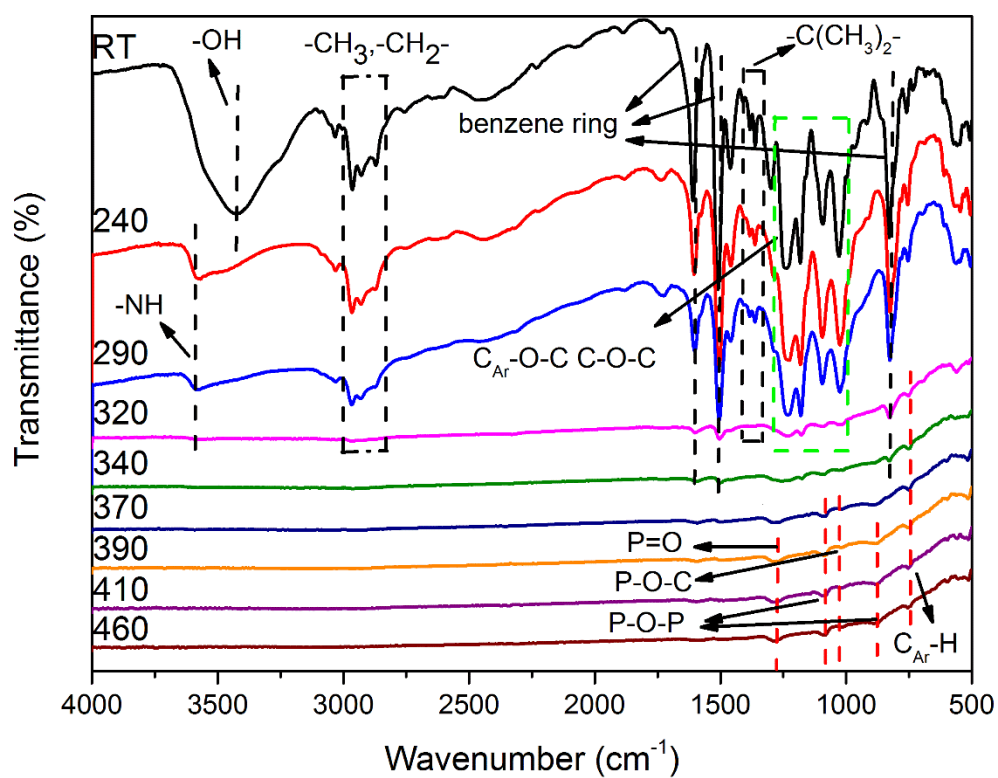
Figure 11 RT-FTIR spectra of EP-4 at different temperature
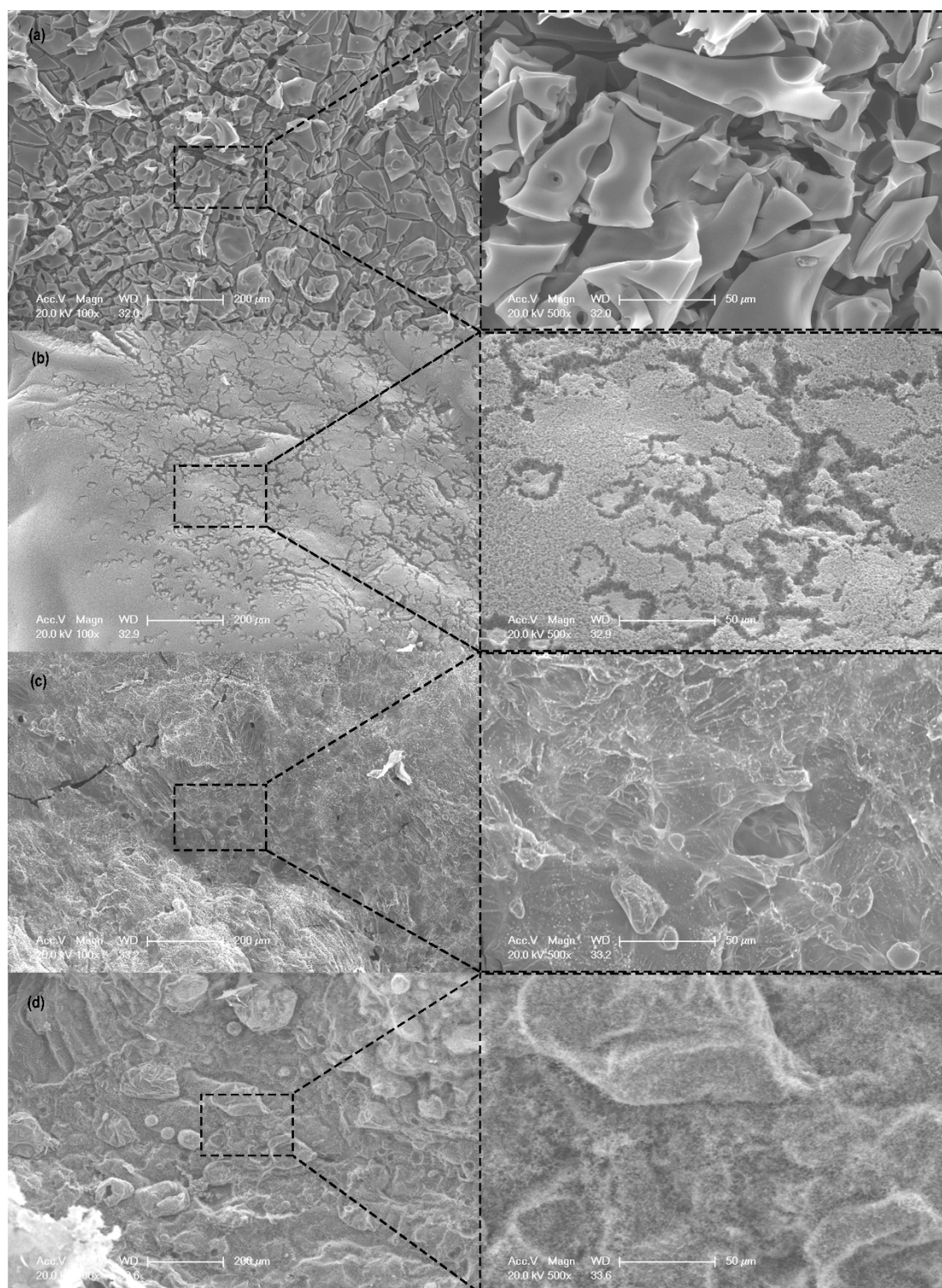
Figure 12 SEM photographs of EP (a), EP-1 (b), EP-2 (c) and EP-4 (d)
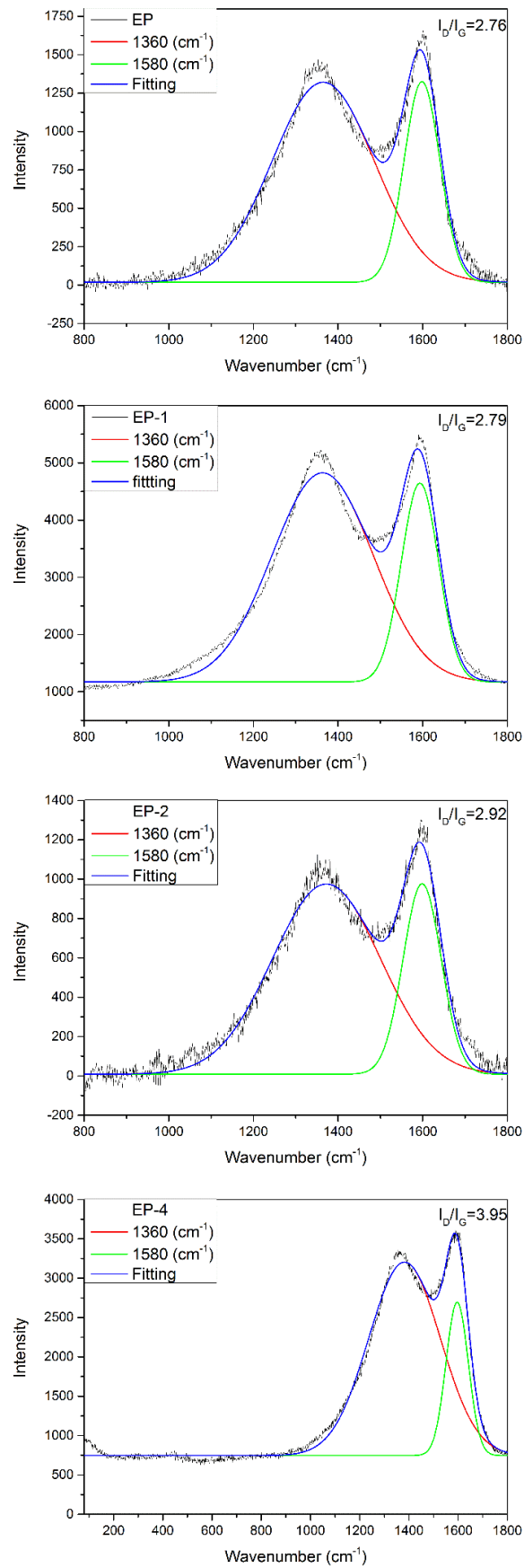
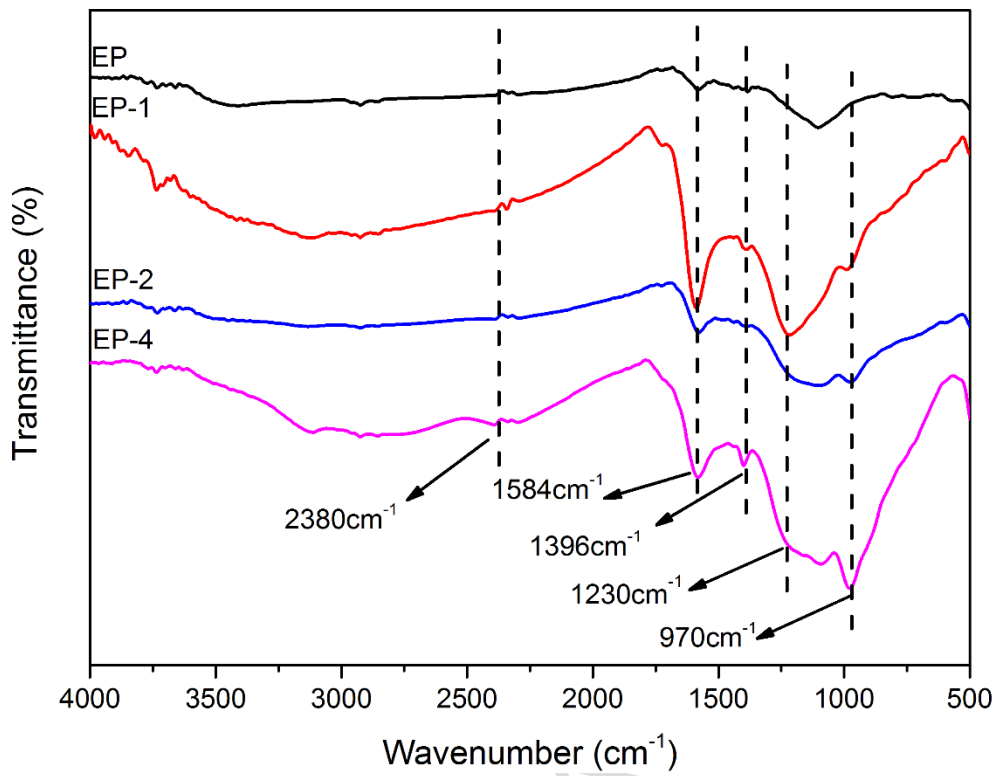Figure 5 Raman spectra of char residues of EP and EP/PPAP composites

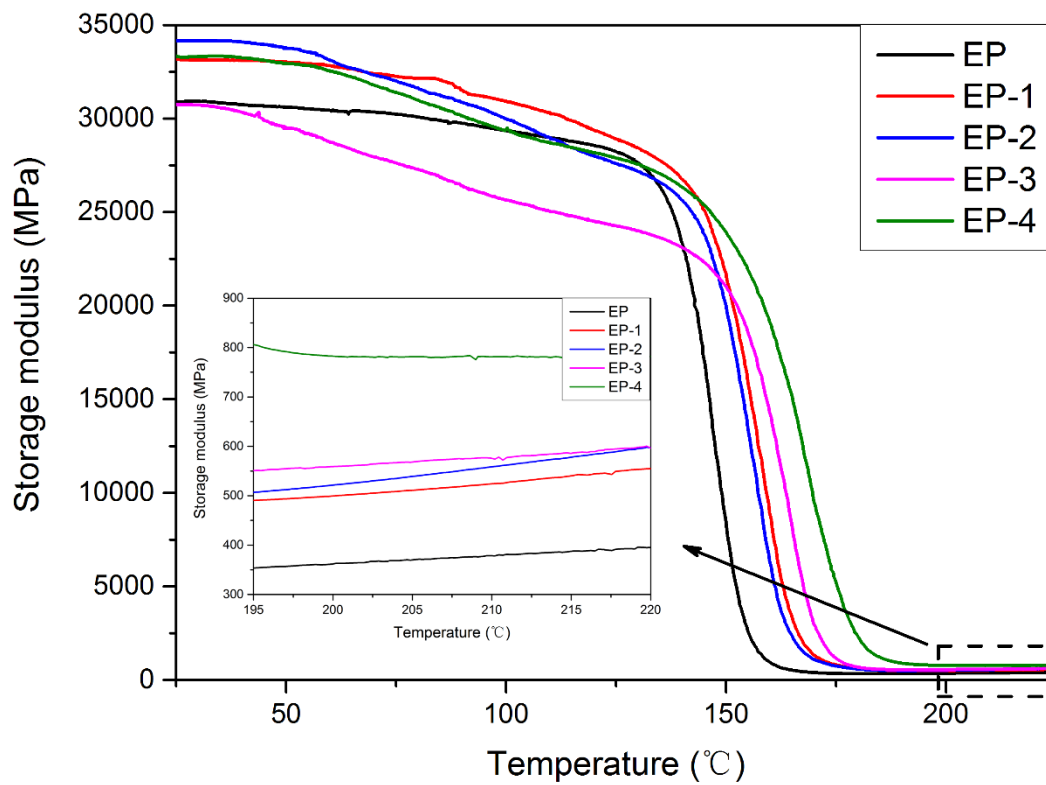Figure 6 FT-IR spectra of char residues after cone calorimetry

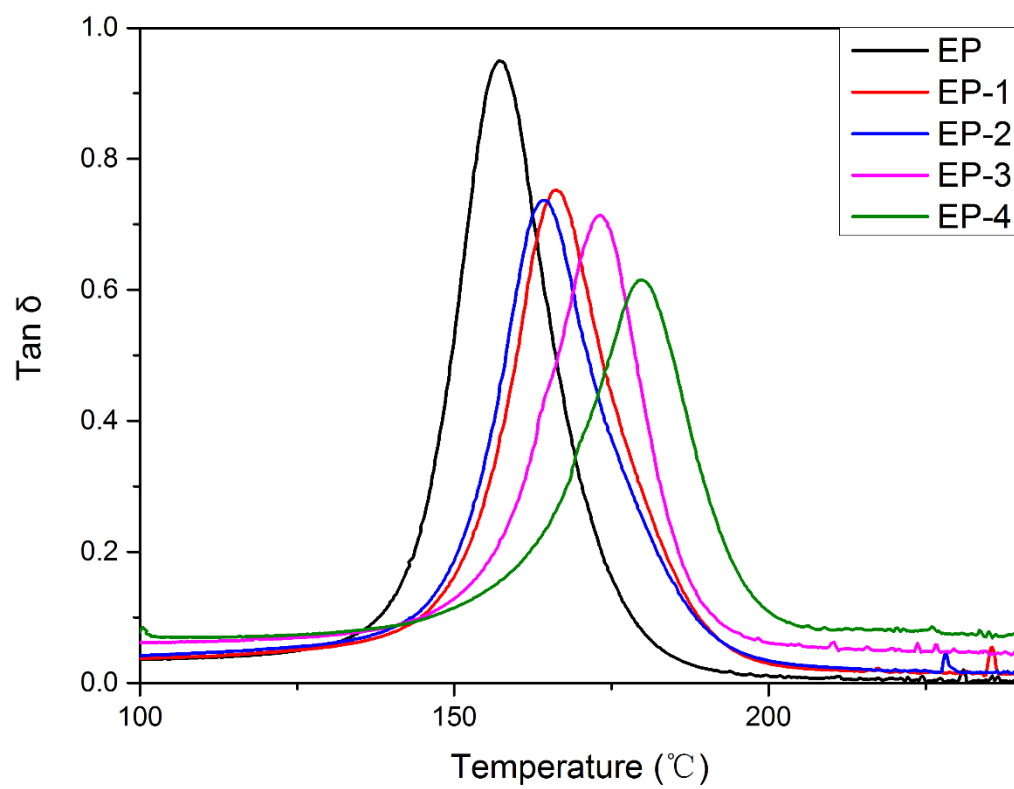Figure 7 Storage curves of EP and EP/PPAP composites

Figure 8 Tanδ curves of EP and EP/PPAP composites

Highlights

1. A novel flame retardant can enhance the char-forming ability of epoxy resin.
2. HRR and THR of the flame retardant epoxy resins were drastically decreased.
3. Improved mechanical properties and glass transition temperatures can be observed.